PEIJIE LOU
CHENGJIE LI
SHULING LIANG
MINGMING FENG
and
BIN PAN

Numerical simulation study on failure characteristics of coal-rock combination with fracture

This paper studies characteristics of deformation failure and fracture growth of fractured coal-rock combination with RFPA2D numerical analysis software. Peak strength of the combination increases with increase of the dip of fracture and the peak strength when dip of fracture is 90° approaches to the peak strength without fracture. Under the same dip of fracture, peak strength of the combination when fracture is in the rock is higher than that in the coal, and fracture in the coal has more significant effect on the strength of the combination than in the rock. If fracture locations in combination are different, the characteristics of fracture growth are different. If dips of fracture in the same location are different, the fracture growth characteristics are different, too. However, fracture growth connection in coal is the main cause of overall failure of the combination body. During the loading, sound emission appears in two ends of fracture and the new fracture in the rock in upper end of the fracture, which mainly is caused by tensile failure. While in the coal, the new fracture in the end of fracture is caused by tensile failure; failures in other part are caused by both tensile failure and shear failure.

Keywords: *Combination body, connected fissure, RFPA2D, sound emission.*

1. Introduction

Social and economic growth has close relationship with development of coal industry. Coal-rock compound layer is usual for mining [1-5], which is different from single coal layer or rock mass. Therefore, it is essential to study deformation failure and strength characteristics of coal-rock combination body. Many professional scholars have taken several studies and get rich achievements [6-9]. Zhang studied and found failure of the combination body test-piece mainly concentrates in the coal and has no relationship with the combination and loading touch way. Aggravation on fracture growth and failure degree of the coal can induce to some degree in fracture or failure of the rock [10]. Fu, by using finite element RFPA2D simulation software [11,12], gets the similar results and analyzed mechanical properties and sound emission characteristics of coal-rock combination body under different dips of fracture and confining pressures [13,14].

It is obvious that strength of both coal and rock in the combination body can influence overall buckling failure of the combination body. Liu found that if the rock strength is lower, fracture of the combination body test-piece will grow to the rock and the rock suffers tensile failure; if the rock strength is higher, the failure mainly is in the coal [15]. Zhao established the coal-rock combination body model with different types to research stress-strain relationship and shear failure characteristics under different confining pressures [16].

Besides static loading, Dou took test on burst orientation of coal-rock combination body, and found that if coal sample percentage increases, elasticity modulus and burst energy index of combination body test-piece decrease gradually, and elastic energy index increases gradually. The burst energy index can increase with increase of height ratio of roof and coal sample [17]. Acoustic emission occurs during rock failure. [18-24]. Xiao studied sound emission characteristics and burst orientation rules of coal, rock, and coal-rock combination body, and got the conclusion that rock has great effect on mechanical properties and burst orientation of the coal in combination body [25]. Liu used improved Hopkinson bar to develop test research on dynamic failure characteristics of coal-rock combination body under one-dimensional dynamic and static load [33]. For mechanical properties of coal-rock combination body under graded loading/unloading, Zuo et al., (2011) [26] and Zhu et al., (2016) [27] got the conclusion: failure of the combination body mainly is brittle failure mechanism; failure of the combination body under graded loading/unloading is more fractured by comparing with single-axial effect. In addition, the former compared differences and same points of failure models and mechanical behaviours of rock, coal, and combination body under single-

Messrs. Peijie Lou, Chengjie Li, Shuling Liang, Mingming Feng and Bin Pan, School of Civil and Architectural Engineering, Anhui University of Science and Technology, Huainan 232001, and Mr. Peijie Lou is also with Opening Laboratory for Deep Mine Construction, Henan Polytechnic University, Jiaozuo 454000, Center for Post-Doctoral Studies of Civil Engineering, Anhui University of Science and Technology, Huainan 232001, Engineering Research Center of Underground Mine Construction, Ministry of Education, Anhui University of Science and Technology, Huainan 232001, China. Email: 651832861@qq.com

Table 1 Relevant parameters of model material

Material	Uniaxial compressive strength		Young's elastic modulus		Poisson ratio		Internal friction angle/°	T-C ratio
	Coefficient of homogeneity	Microscopic average value /MPa	Coefficient of homogeneity	Microscopic average value /MPa	Coefficient of homogeneity	Microscopic average value		
Coal	5	20	6	6,500	10	0.30	30	10
Sandstone	10	60	10	30,000	10	0.25	30	10

Table 2 The strength of fractured combination body for different types

Fracture location	Peak strength				Residual strength			
	30°	45°	60°	90°	30°	45°	60°	90°
Rock	7.70	8.07	8.66	8.83	0.54	0.49	0.90	0.89
Coal	4.52	5.09	5.72	8.67	0.68	0.72	0.98	0.81

axial and three-axial stresses [28]. Guo took simulation study on single-axial compression test results of the combination body with 4 different dips of fracture by using extended finite element. He found external work, yield stress, and elastic strain can decrease when the dip of fracture increases from 0° to 60°, while it can depart when the dip of fracture exceeds 45°~50°. It can be used as critical sign for coal-rock combination body changing from shear deformation failure mechanism into interface slippage failure mechanism [29]. All above are parts of various achievements and there are still some more achievements on relevant fields.

However, during roadway excavation or coal mining, the coal-rock combination body can suffer some fractures due to failures, and the fractures can cause effect on mechanical properties of the combination body [30-32]. The site test is difficult and test in lab is complex, so it will give numerical simulation study on deformation failure and fracture growth of fractured coal-rock combination rock under single-axial compression.

2. Establishment of numerical model

Simulation software used for the test is RFPA2D (rock failure process analysis) researched and developed by Northeastern University. The software can be used for various engineering matters such as rock rheology analysis, slope stability simulation analysis, gas outburst of coal-rock combination body, gas-solid coupling, underground excavation and support, etc. Matters mentioned in this paper are rock test-piece loading deformation failure and sound emission.

Dimension of this numerical model is 100 mm×50 mm (height×width), having 200×100 (line×row) units. The combination body contains sandstone in upper and coal in lower with ratio of half-to-half. The junction surface is formed naturally. Fracture in the model is 20mm (length) and 1mm (width) in four different locations in coal and rock. Dips of fracture θ of the locations are 30°, 45°, 60° and 90° respectively, and the fracture layout in the combination body (Fig.1). Calculation model in this paper is control displacement single-axial loading with 0.002mm for each step. During the test, the load step is set as 400 to ensure getting complete failure curve of the test-piece. Both coal and rock adopt two-shear failure model, relevant parameters of the model can be seen in Fig.1. When taking the simulation calculation, it is deemed that the complete failure is reached when peak load of the combination body reaches the residual strength.

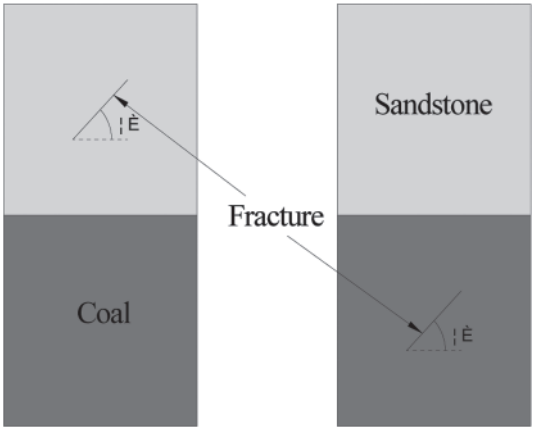

Fig.1 Diagram of fractured coal-rock combination body

3. Calculation result and analysis

3.1 Analysis on strength and deformation characteristics of fractured combination body

3.1.1 Fracture is in the rock

Before calculating the fractured combination body, it shall take analog computation for complete coal-rock combination body without fracture, peak strength and residual strength of which is 8.84 MPa and 0.99 MPa respectively. Analysis on calculation results of peak strength, peak stress, and residual strength of fractured combination body is given in Tables 1 and 2.

If fracture is in upper rock, curves of stress-load step are nearly linear before reaching the peak (Fig.2(a)) of which, "complete body" means complete coal-rock combination body without fracture, "upper-30" means fracture is in rock

and the dip of fracture is 30°, and "upper-30-25" means fracture is in rock, dip of fracture is 30° and current load step is 25, and so on. It is obvious that peak strength of combination body increases gradually when the dip of fracture increases. When the dip of fracture is 60°, peak strength and residual strength of the combination body are similar with complete body. When the dip of fracture is 90°, curves of axial stress-load step almost coincide with that of the complete body. It means if the dip of fracture is larger when fracture is in rock, effect on strength and deformation of the combination body will be smaller. For two combination bodies with smaller dips of fracture, curves of axial stress-load step almost coincide with each other after the 50th load step. When it is under complete failure, deformations of the combination body when dip of fracture is 30° and 45° are greater than that under 60° and 90° (deformation is in direct proportion to load step).

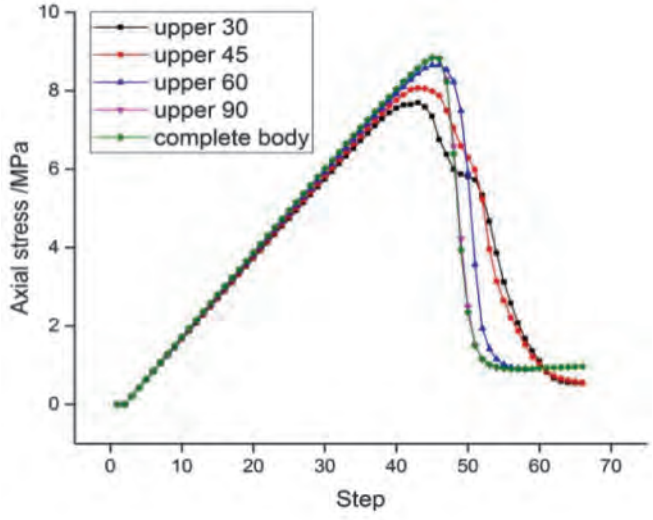

(a) Fissures locate in the rock mass

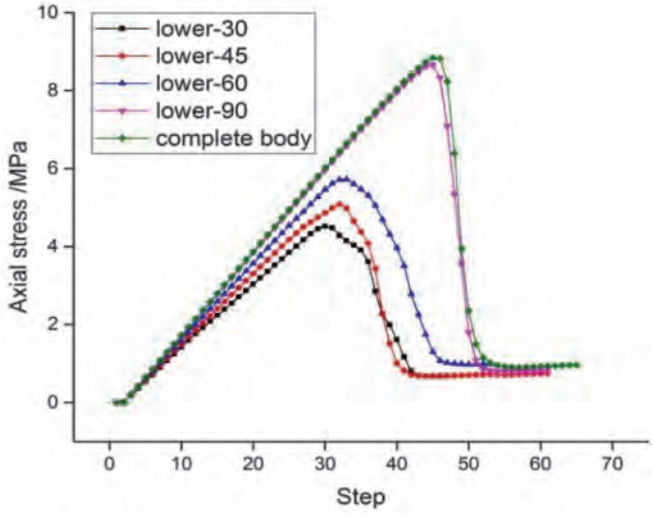

(b) Fissures locate in the coal

Fig.2 The curves of stress-load step of fractured coal-rock combination body

3.1.2 Fracture is in the coal

When fracture is in coal in lower part, curves of axial stress-load step is linear at the beginning of the peak and curves with smaller dips of fracture derivate from original direction soon with new linear. Peak strength of the combination body increases with increase of dip of fracture. The amplification is small when dip of fracture changes between 30° and 60° and larger between 60° and 90°, and it increases to 8.67 MPa at 90° from 4.52 MPa at 30°, which is higher than scope of peak strength of upper fractured combination body (Fig.2). With increase of dip of fracture, deformation of the combination body under compete failure reaching residual strength increases continuously, which is inverse with situation of upper fractured combination body. When it is under final failure, residual strengths of combination body under four different dips of fracture are similar.

3.2 Analysis on model failure and fracture propagation

3.2.1 Fracture is in the rock

It can know from above description that no matter the fracture is in coal or rock, strength of the combination body increases with increase of the dip of fracture, but the increase rule is different. For fracture combination body with the same dip of fracture, peak strength is higher when the fracture is in rock, which means fracture in the coal has great effect on strength of the combination body. It can be known from data in Fig.2 that the effect will be greater if the dip of fracture is smaller.

As shown in Fig.3(a), when dip of fracture is 30°, coal in lower part will be "fatter" than rock in upper part during loading due to different poisson ratio of the rock and coal. It means poisson of coal is more obvious, which is related to parameter set of model material and meets the actual situation. Two ends of fracture will suffer the stress concentration and then form new fractures synchronously, see red circle in the Fig.3. The new fracture is vertical with original fracture at the beginning and then grows in axial direction. The lengths of new fractures in two ends of fracture are similar during growth. When it reaches certain length, new fracture in upper end grows slowly in the length and new fracture in lower end

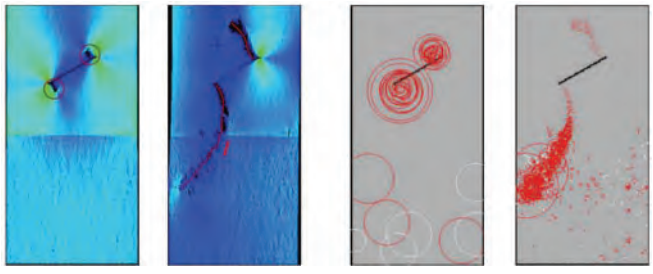

(a) Shear stress diagrams (b) Acoustic emission diagrams

Fig.3 Deformation and failure diagrams of the upper-30 combination body

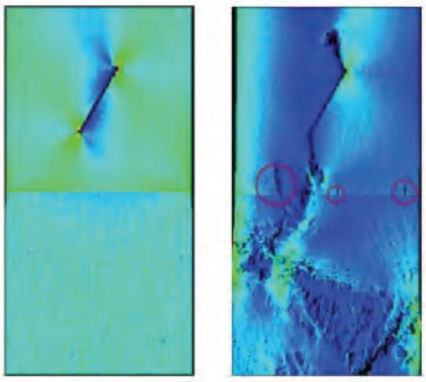

Fig.4 The shear stress diagrams of the upper-60 combination body

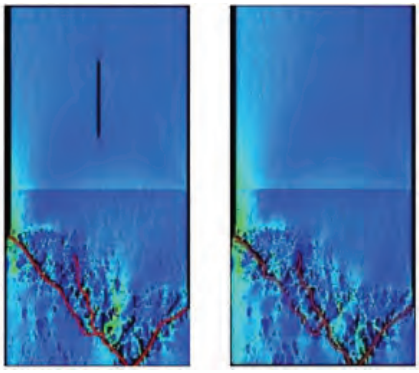

Fig.5 The comparison between upper-90-50 body and complete body (under the same load step)

grows downward, crosses the junction surface and forms an arc connected fissure l in upper left part of the coal. Finally, it can cause buckling failure of the combination body so that rock in upper part is broken along growth direction of new fracture in upper end of original fracture. Before growing to the junction surface, new fractures in two ends of original fracture are caused by tensile failure, and the coal suffers both tensile failure and shear failure when new fractures in lower end grows to the coal. It can be known from Fig.3(b), besides connected fissure caused by fracture growth in lower end of original fracture, other part of the coal has little shear and tensile failure. The white circle shows the sound emission caused by shear failure under current step, and the red circle shows the sound emission caused by tensile failure under current step.

When dip of fracture is 45°, failure characteristic of the combination body is similar with that when the dip of fracture is 30°, so it is not repeated here. In Fig.4, the 35th step causes no great fracture when dip of fracture is 60°. It can be known that, comparing to condition when the dip of fracture is 30°, length of new fracture under the same step is short, but quantity of connected fissure under complete failure of coal is more and degree of crushing of the coal is more serious. When the composition body is under complete failure, new fracture in upper end of original fracture fails to grow to upper end of the rock and it is the coal failure causes overall failure

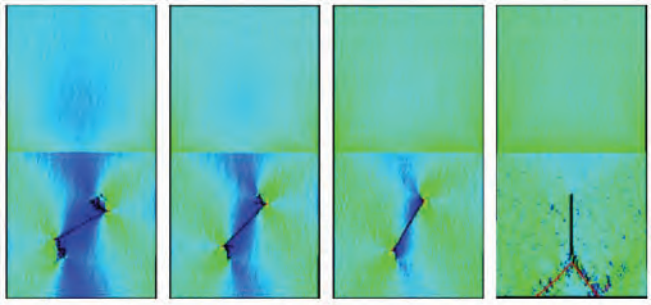

(a) Shear stress diagrams in loading

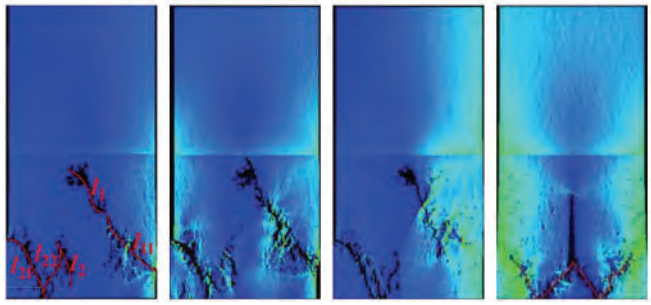

(b) Shear stress diagrams at failure

Fig.6. Shear stress diagrams of coal-fractured combination body

of combination body. It can be seen from Fig.5, in addition, if failure appears for composition containing above three dip of fractures in the coal, rock in junction surface can appear little fractures, circled in red in Fig.4. When the dip of fracture is 90°, failure appears firstly in coal in lower part and then forms two connected fissures along with the load, the failure can be tensile and shear failure. While rock in upper part has no obvious new fracture and is same with failure mode of the overall combination body. Therefore, vertical fracture in upper part has little effect on deformation and failure of the combination body.

3.2.2 Fracture is in the coal

Fig.6(a) shows shearing forces of coal fracture combination body with different dips of fracture during loading. When the load step is same, new fracture lengths under the first three dips of fracture will decrease with increase of dip of fracture. It can be known from Fig.6(b) that: when fracture is in the coal, it is similar with situation when fracture is in upper part and tensile fracture is formed in two ends of fracture due to stress concentration under the other three dips of fracture except 90º. The new fracture in upper part of original fracture grows into fracture l1 to the junction surface, stops growth to the rock and does not cause failure of junction surface when approaches to the junction surface, but forms a fracture l11 crossing the coal in reverse direction of growth of wing fracture in the end. New fracture in lower part forms l2 by growing in the coal and forms the connected fissures l21 and l22 in lower left corner, which are parallel to the connected fissure in upper part. When dip of fracture is 90º, no long new fracture forms in upper end of original fracture when the combination body is under failure, but a

reversed V-type connected fissure forms in the lower end, which becomes W-type after several load steps. Factually, when the combination body is pressured and before connected fissure forms in lower coal, other part of the coal suffers many sound emissions. In consideration of that failure quantity of rock and sound emission is in direct proportion to quantity of failure element (Tang, 1997), other parts also suffer severe failure. In conclusion, the upper rock is perfect all the time during loading and damaging, and combination body failures under four dips of fracture are caused by failure of lower coal.

3. Conclusions

1. When fractures are in the same location, peak strength of the coal-rock combination body will increase with increase of fracture dip of fracture and will approach the strength without fracture. If the fracture dip of fracture is same, the peak strength is higher when fracture is in the rock.
2. When fractures are in different locations and the fracture growth characteristics are different: growth of new fracture in the end under fracture with different dips of fracture cause connected fissure of the coal if the fracture is in the rock so that it is under failure. It approaches to the value without fracture with dip of fracture is 90º and only the coal is under failure. If the fracture is in the coal, connected fissure is formed to cause failure of the combination body so that the rock is under failure completely. Failure of coal is the main cause for the combination body failure.
3. During loading, acoustic emission appears in two ends of the fracture firstly with tensile fracture, new fracture in the mass forms in upper end of original fracture, and the new fracture suffers tensile fracture. While in the coal, only new fracture starting from end of the fracture is tensile fracture and all others are combination body of tensile and shear fracture.

Acknowledgements

This paper is supported by Anhui Provincial Natural Science Foundation (1608085QE122); Opening Laboratory for Deep Mine Construction, Henan Polytechnic University (2015KF-05); China Postdoctoral Science Foundation (2016M590558); The Open Project Program Foundation of Engineering Research Center of underground mine construction, Ministry of Education(Anhui University of Science and Technology) (2015KF04); Graduate innovation fund of Anhui University of Science and Technology(2017CX2011,2017CX2078).

References

1. Zuo J. P., Wang Z. F., Zhou H. W., Pei J. L., Liu J. F., (2013): "Failure behavior of a rock-coal-rock combined body with a weak coal interlayer," *International Journal of Mining Science and Technology*, vol. 23, no. 6, pp. 907-912,.
2. Zhao Z. H., Wang W. M., Wang L. H., Dai C. Q., (2015): "Compression-shear strength criterion of coal-rock combination model considering interface effect," *Tunnelling and Underground Space Technology*, vol. 47, pp. 193-199.
3. Yu W. J., Feng T., Wang W. J., Liu H., Ma P. Y., Wang P., Li R. H., (2014): "Deformation mechanism, control principle and technology of soft half coal rock roadway," *Chinese Journal of Rock Mechanics and Engineering*, vol. 33, no. 4, pp. 658-671.
4. Jin G., Wang L. G., Li Z. L., Zhang J. H., (2015): "Study on the gateway rock failure mechanism and supporting practice of half-coal-rock extraction roadway in deep coal mine," *Journal of Mining & Safety Engineering*, vol. 32, no. 6, pp. 963-967.
5. Li J. F., Guo W. Y., Zhang C. L., Cheng C. X., Liu J. K., Zhou G.L. (2013): "Supporting technology of fully mechanized half-coal rock mining roadway in thin seam," *Safety in Coal Mines*, vol. 44, no. 12, pp. 97-99+103.
6. Jiang Y. D., Wang T., Song Y. M., Wang X., Zhang W., (2013): "Experimental study on the stick-slip process of coal-rock composite samples," *Journal of China Coal Society*, vol. 38, no. 2, pp. 177-182.
7. Zhao S. K., Zhang Y., Han R. J., Jiang H. B., Zhang N. B., Xu Z. J. (2013): "Numerical simulation experiments on bursting liability evolution of compound coal-rock structure," *Journal of Liaoning Technical University (Natural Science)*, vol. 32, no. 11, pp. 1441-1446.
8. Jing L. W., Wang Q. C., Yao W. J, Li Z. W. (2017): "Research on supporting technology with "short anchor+light frame" for coal roadway with broken roof," *Coal Technology*, vol. 36, no. 3, pp. 6-8.
9. Zhang Y. W. (2016): "Study on support system optimization of broken seam and rock gateway along fault," *Coal Science and Technology*, vol. 44, no. 9, pp. 72-76+166.
10. Zhang Z. T., Liu J. F., Wang L., Yang H. T., Zuo J. P. (2012): "Effects of combination mode on mechanical properties and failure characteristics of the coal-rock combinations," *Journal of China Coal Society*, vol. 37, no. 10, pp. 1677-1681.
11. Li L. C., Tang C. A., Zhu W. C., Liang Z. Z. (2009): "Numerical analysis of slope stability based on the gravity increase method," *Computers and Geotechnics*, vol. 36, no. 7, pp. 1246-1258.
12. Tang C. A., Tang S. B. (2011): "Applications of rock failure process analysis (RFPA) method," *Journal of Rock Mechanics and Geotechnical Engineering*, vol. 3, no. 4, pp. 352-372.
13. Fu B., Zhou Z. H., Wang Y. X., Liu S., Xiao Y. C. (2016): "Numerical simulation of different combination of coal

and rock sample mechanics and acoustic emission characteristics," *Journal of Nanjing University of Science and Technology*, vol. 40, no. 4, pp. 485-492.

14. Fu B., Zhou Z. H., Wang Y. X., Yin X., Liu S., Xiao Y. C. (2016): "Numerical simulation of coal-rock combination body failure process by RFPA2D," *Journal of Dalian University of Technology*, vol. 56, no. 2, pp. 132-139.
15. Liu J., Wang E. Y, Song D. Z., Yang S. L., Niu Y. (2014): "Effects of rock strength on mechanical behavior and acoustic emission characteristics of samples composed of coal and rock," *Journal of China Coal Society*, vol. 39, no. 4, pp. 685-691.
16. Zhao Z. H., Wang W. M., Dai C. Q., Yan J. X. (2014): "Failure characteristics of three-body model composed of rock and coal with different strength and stiffness," *Transactions of Nonferrous Metals Society of China*, vol. 24, no. 5, pp. 1538-1546.
17. Dou L. M., Lu C.P., Mu Z. L., et al. (2006): "Rock burst tendency of coal-rock combinations sample," *Journal of Mining & Safety Engineering*, no. 1, pp. 43-46,.
18. Xu J., Li S. C., Tao Y. Q., Tang X. J., Wu X. (2009): "Acoustic emission characteristic during rock fatigue damage and failure," *Procedia Earth and Planetary Science*, vol. 1, no. 1, pp. 556-559.
19. Zhang X. P., Zhang Q., Wu S. C. (2017): "Acoustic emission characteristics of the rock-like material containing a single flaw under different compressive loading rates," *Computers and Geotechnics*, vol. 83, pp. 83-97.
20. Fan J. Y., Chen J., Jiang D. Y., Chemenda A., Chen J. C., Ambre J. (2017): "Discontinuous cyclic loading tests of salt with acoustic emission monitoring," *International Journal of Fatigue*, vol. 94, pp. 140-144.
21. Kwiatek G., Plenkersb K., Martínez-Garzón P., Leonhardt M., Zang A., Dresen G. (2017): "New insights into fracture process through in-situ acoustic emission monitoring during fatigue hydraulic fracture experiment in Äspö hard rock laboratory," *Procedia Engineering*, vol. 191, pp. 618-622.
22. Filipussia D. A., Guzmána C. A., Xargayc H. D., Hucailuka C., Torresa D.N. (2015): "Study of acoustic emission in a compression test of andesite rock," *Procedia Materials Science*, vol. 7, no. 9, pp. 292-297.
23. Wu Y. L., Chen J., Zeng S. M. (2011): "The acoustic emission technique research on dynamic damage characteristics of the coal rock," *Procedia Engineering*, vol. 26, pp. 1076-1082.
24. Liang Y. P., Li Q. M., Gu Y. L., Zou Q. L. (2017): "Mechanical and acoustic emission characteristics of rock: Effect of loading and unloading confining pressure at the postpeak stage," *Journal of Natural Gas Science and Engineering*, vol. 44, pp. 54-64.
25. Xiao X. C., Jin C., Pan Y. S., Ding X., Zhao X., Xu J. (2016): "Experimental study on acoustic emission characteristic and outburst-proneness of coal-rock combinations during failure process," China Safety Science Journal, vol. 26, no. 4, pp. 102-107.
26. Zuo J. P., Xie H. P., Meng B. B., Liu J. F. (2011): "Experimental research on loading-unloading behavior of coal-rock combination bodies at different stress levels," *Rock and Soil Mechanics*, vol. 32, no. 5, pp. 1287-1296,.
27. Zhu Z. H., Feng T., Gong F. Q., Ye Z. Y., Yu Z. (2016): "Experimental research of mechanical properties on grading cycle loading-unloading behavior of coal-rock combination bodies at different stress levels," *Journal of Central South University (Science and Technology)*, vol. 47, no. 7, pp. 2469-2475.
28. Zuo J. P., Xie H. P., Wu A. M., Liu J. F. (2011): "Investigation on failure mechanisms and mechanical behaviors of deep coal-rock single body and combined body," *Chinese Journal of Rock Mechanics and Engineering*, vol. 30, no. 1, pp. 84-92.
29. Guo W. Y., Zhou H., XU N. H., Chen W. G, Wei P. (2016): "Simulation study of mechanical properties of coal rock combination," *Safety in Coal Mines*, vol. 47, no. 2, pp. 33-35+39,.
30. PU C. Z., Cao P. (2012): "Failure characteristics and its influencing factors of rock-like material with multi-fissures under uniaxial compression, *Transactions of Nonferrous Metals Society of China*, vol. 22, no. 1, pp. 185-191,.
31. Wu J. Y., Feng M. M., Yu B. Y., Han G. S. (2017): "The length of pre-existing fissures effects on the mechanical properties of cracked red sandstone and strength design in engineering," *Ultrasonics*, vol. 82, pp. 188-199.
32. Chen L. Y., Liu J. J. (2015): "Numerical analysis on the crack propagation and failure characteristics of rocks with double fissures under the uniaxial compression," *Petroleum*, vol. 1, no. 4, pp. 373-381,.
33. Liu S. H., Qin Z. H., Lou J. F. (2014): "Experimental study of dynamic failure characteristics of coal-rock compound under one-dimensional static and dynamic loads," *Chinese Journal of Rock Mechanics and Engineering*, vol. 33, no. 10, pp. 2064-2075.